Age-related changes in the intrinsic functional connectivity of the human ventral vs. dorsal striatum from childhood to middle age

James N. Porter[a], Amy K. Roy[d], Brenda Benson[e], Christina Carlisi[e], Paul F. Collins[b], Ellen Leibenluft[e], Daniel S. Pine[e], Monica Luciana[b,c], Monique Ernst[e,*]

[a] University of Iowa Hospitals and Clinics Department of Neurology, USA
[b] University of Minnesota Department of Psychology, USA
[c] University of Minnesota Center for Neurobehavioral Development, USA
[d] Fordham University, Department of Psychology, USA
[e] Section on Development and Affective Neuroscience, National Institute of Mental Health, National Institutes of Health, USA

ARTICLE INFO

ABSTRACT

The striatum codes motivated behavior. Delineating age-related differences within striatal circuitry can provide insights into neural mechanisms underlying ontogenic behavioral changes and vulnerabilities to mental disorders. To this end, a dual ventral/dorsal model of striatal function was examined using resting state intrinsic functional connectivity (iFC) imaging in 106 healthy individuals, ages 9–44. Broadly, the dorsal striatum (DS) is connected to prefrontal and parietal cortices and contributes to cognitive processes; the ventral striatum (VS) is connected to medial orbitofrontal and anterior cingulate cortices, and contributes to affective valuation and motivation. Findings revealed patterns of age-related changes that differed between VS and DS iFCs. We found an age-related increase in DS iFC with posterior cingulate cortex (pCC) that stabilized after the mid-twenties, but a decrease in VS iFC with anterior insula (aIns) and dorsal anterior cingulate cortex (dACC) that persisted into mid-adulthood. These distinct developmental trajectories of VS vs. DS iFC might underlie adolescents' unique behavioral patterns and vulnerabilities to psychopathology, and also speaks to changes in motivational networks that extend well past 25 years old.

1. Introduction

The basal ganglia, at the intersection of the midbrain and forebrain, are implicated in a wide range of motor, cognitive, and affective functions that are subserved by cortical–striatal–thalamic–cortical loops (Alexander et al., 1986; Haber, 2003; Selemon and Goldman-Rakic, 1985). Accordingly, the striatum, the major input component of the basal ganglia, receives connections from all cortical regions in a parallel, segregated fashion. Five parallel networks were originally proposed in the classic paper by Alexander et al. (1986); more recent accounts add the notion of a functional gradient within the striatum (Haber, 2003). Specifically, a ventral to dorsal schema has been linked with an affective/motivational to cognitive/motor

* Corresponding author at: Head of Neurodevelopment of Reward Systems, Emotional Development and Affective Neuroscience Branch (EDAN), Section on Neurobiology of Fear and Anxiety (NFA), National Institute of Mental Health/NIH, 15K North Drive, Bethesda, MD 20892, USA.
Tel.: +1 301 402 9355; fax: +301 402 2010; mobile: +1 301 675 4525.
E-mail address: ernstm@mail.nih.gov (M. Ernst).

gradient with relevance to various aspects of behaviors (e.g., learning, reward responses, goal-directed or habitual actions) (Fareri et al., 2008; Haber, 2003; Liljeholm and O'Doherty, 2012; O'Doherty et al., 2004; Voorn et al., 2004). Anatomically, the ventral striatum typically includes the nucleus accumbens (NAcc) and ventral regions of the caudate nucleus and putamen, and the dorsal striatum includes the dorsal regions of the putamen and caudate nucleus.

The striatal functional gradient is reminiscent of the dual neural systems model of adolescent behavior, which focuses on the interaction between cognitive and motivational neural systems that influence overt behavioral patterns (Casey et al., 2008; Hardin and Ernst, 2009; Luciana et al., 2012; Steinberg, 2010). Dual neural systems models have been formulated to account for risk-taking and sensation-seeking behaviors, which are particularly prominent and often worrisome in adolescence (Minino, 2010; Spear, 2000; Steinberg et al., 2008). These models theorize that different developmental trajectories of the cognitive and motivational networks are responsible for these behaviors (Casey et al., 2008; Galvan et al., 2006; Harden and Tucker-Drob, 2011; Luciana et al., 2012). Specifically, recent formulations suggest that a strong neural responsivity of the motivational system together with a progressively maturing cognitive system in adolescence sets up a dynamic state that leaves emotions and associated motivational drives insufficiently modulated by cognitive control (Ernst et al., 2006; Luciana et al., 2012; Steinberg, 2010). This dual-system model suggests that the transition from adolescence into adulthood might be marked by distinct ontogenic changes in ventral versus dorsal striatum.

A convincing literature from the fields of psychology and neuroimaging provides support for the dual-system theory, both at a behavioral (Harden and Tucker-Drob, 2011; Steinberg et al., 2008; Urosevic et al., 2012) and a neural level (Chein et al., 2011; Ernst et al., 2005; Galvan et al., 2006; Somerville et al., 2010; Van Leijenhorst et al., 2010; but see Bjork et al., 2004, 2010). For example, the ventral striatum, a key component of the motivational system, has been shown to be activated by reward contexts more strongly in adolescents than in adults (Chein et al., 2011; Ernst et al., 2005; Galvan et al., 2006; but see Bjork et al., 2004, 2010). In contrast, during decision-making (but not necessarily in other tasks, such as inhibitory control tasks, e.g., Ordaz et al., 2013), prefrontal cortical regions have been shown to be less activated in adolescents than in adults (Eshel et al., 2007; Galvan et al., 2006; Somerville et al., 2010). The greater activity of the ventral striatum together with the lower activity of the prefrontal cortex during reward-related decision-making in adolescence theoretically sets the stage for risk-taking behaviors. Moreover, from a behavioral standpoint, the transition from adolescence to adulthood witnesses a shift in this balance, characterized by decreasing motivational drives from an over-exuberant state and increasing cognitive control to reach maturation (Luciana and Collins, 2012; Luciana et al., 2005; Luna et al., 2004; Urosevic et al., 2012). However, existing studies only partly resonate with the neural systems framework, in the sense that they capture local age-related differences (regional activations), while failing to reveal how the networks themselves (i.e., collection of functionally connected nodes) work in concert to contribute to different patterns of information processing in adults vs. adolescents. In addition, neuroimaging studies of reward processes that have compared adolescents to adults have not shown clear distinctions between the contributions of ventral vs. dorsal striatum to age-related differences in reward processes (see review, Richards et al., 2013). We now have the methodology and analytic methods to examine and dissociate these networks using resting state intrinsic functional connectivity (iFC; Raichle et al., 2001).

The present study examines age-related differences in ventral striatal (VS) iFC and dorsal striatal (DS) iFC. This approach permits us to define and contrast the VS iFC and DS iFC networks, which are broadly linked to motivation and cognitive function, respectively (Haber, 2003), and to examine the influence of age on these systems. Resting-state iFC reflects phasic activity coupling between regions in an idle state. It is thought to provide a measure of both the history of use of a connection (more use may strengthen iFC; Buckner and Vincent, 2007) and the network's readiness to respond when challenged (Deco et al., 2011). Accordingly, we would expect generally a more strongly linked motivation network and a less strongly linked cognitive network in adolescents compared to adults.

In this study, we examined iFC of the VS and DS across the whole brain in a sample of 106 healthy individuals spanning the ages of 9–44 years. In keeping with the extant literature, we expected to observe a segregation of functional connections for each striatal region regardless of age, such that DS would be more strongly connected with higher cortical association areas in the frontal and parietal lobes, while VS would be more strongly connected with the ventral prefrontal cortex (PFC), the amygdala, midbrain, and anterior cingulate cortex (Choi et al., 2012; Di Martino et al., 2008). Based on a dual neural systems model (Luciana et al., 2012; Steinberg, 2010) and strong evidence of a decline in VS activation and associated behaviors from adolescence into adulthood (Urosevic et al., 2012), we expected decreasing VS iFC and increasing DS iFC in the transition from adolescence to adulthood. The age at which striatal connectivity changes stabilize is assumed to be in the mid-twenties, given recent structural findings as observed throughout the brain (Giedd et al., 1999; Giorgio et al., 2008; Lebel and Beaulieu, 2011), but no studies have yet reported on striatal iFC in the transition from adolescence to early adulthood and into mid-adulthood.
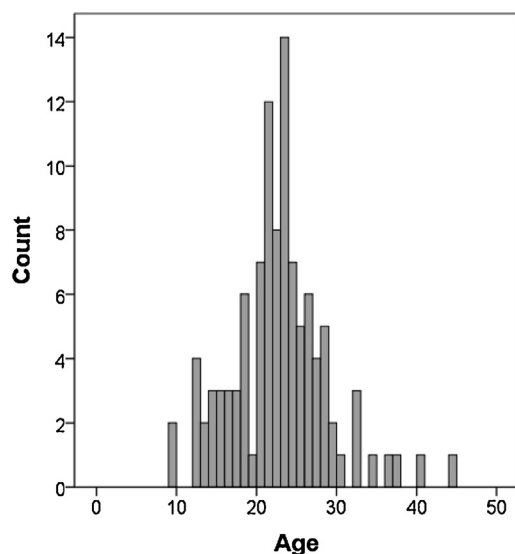
2. Methods

2.1. Participants

One hundred sixty-six healthy participants (75 males, 91 females; 8.5–44.8 years old) completed resting state fMRI scans (with identical parameters) within the context of multiple studies at the same research institution. Clinical assessments using psychiatric interviews (for minors: the Kiddie Schedule for Affective Disorders and Schizophrenia, KSADS; Kaufman et al., 1997; for adults: the Structured Clinical Interview for DSM-IV, SCID; First

Table 1
Demographics of the whole sample and 3 age groups.

	Full sample	9–19.0	19.1–24.9	25+
Males/females	42/64	11/16	18/30	13/18
Age range	9.17–44.17	9.17–18.92	19.00–24.67	25.00–44.17
M(SD)	22.77(6.07)	15.29(2.82)	22.42(1.44)	29.57(4.73)
IQ[a] range	91–139	96–134	91–136	93–139
M(SD)	117.95(10.23)	114.81(10.31)	118.67(9.73)	119.51(10.66)

[a] IQ data not collected for 3 participants in the 19–24 age group.

Fig. 1. Age distribution across the whole sample. Each bar represents a 1-year interval.

et al., 2002), medical history, and physical exams confirmed that all participants were without histories of psychiatric or medical illnesses and were not taking any psychotropic medications. Adult participants and parents of minor participants provided informed consent, and minor participants provided informed assent for the study. The original recruitment studies, as well as the combination of data for purposes of the current study, were approved by the Institutional Review Board of the National Institute of Mental Health.

After fMRI preprocessing and motion-related quality control procedures (see below), 106 participants (42 males, 64 females; 9.17–44.17 years old) were retained for functional connectivity analyses. Table 1 describes the final sample, and Fig. 1 represents a histogram of the age distribution.

2.2. MRI acquisitions and preprocessing

During resting state scans (6 min in duration), participants were instructed to remain still and to keep their eyes open; a white central fixation cross was projected on a black background for the duration of the scans. As the resting state scans were collected in the context of several different research protocols, some participants completed their resting state scans immediately after having performed a cognitive task (N = 73, 25 male, 48 female), and

others after a structural scan or at the outset of the scanning session (N = 30, 16 male, 14 female). To examine whether scan context had an effect upon striatal iFC profiles (i.e., had cognitive task "carryover" effects), we conducted voxelwise t-test analyses to compare these two groups and found no statistically significant group differences (data not shown). Thus, the factor of scan context is not included in the following analyses.

Data were collected at the NeuroMagnetic Resonance Center of the National Institutes of Health on three different General Electric (Waukesha, WI) Signa 3T scanners, with the same acquisition parameters: 180 single-shot EPI volumes; TR = 2000 ms; TE = 30 ms; flip angle = 90, 36 slices, matrix = 64 × 64; FOV = 192 mm; acquisition voxel size = 3 mm × 3 mm × 4 mm. T1-weighted anatomical images were also collected using the same parameters across scanners: SPGR, TE/TI = min full/725 ms, receiver bandwidth = 31.25, flip angle = 6; 124 slices, FOV = 256 mm, voxel dimensions 0.86 mm × 0.86 mm × 1.2 mm.

Image preprocessing was carried out using components of AFNI (http://afni.nimh.nih.gov/afni/) and FSL (www.fmrib.ox.ac.uk). The procedures were similar to those outlined by the 1000 Functional Connectomes Project (http://www.nitrc.org/projects/fcon_1000/), but with modifications unique to this study. This approach is akin to those described in Di Martino et al. (2008) and Roy et al. (2009) (see Supplemental Table S1 for processing and analysis summaries). Preprocessing steps included (1) removal of the first four volumes to allow for steady state magnetization, (2) slice time correction for interleaved acquisitions with FSL's *slicetimer*, (3) 3D motion correction with AFNI's *3dvolreg*, (4) timeseries outlier despiking with AFNI's *3dDespike*, (5) non-brain removal using FSL's *BET* (Smith, 2002), (6) spatial smoothing using a Gaussian kernel of FWHM 6.0 mm, (7) grand-mean intensity scaling, (8) highpass temporal filtering (Gaussian-weighted least-squares straight line fitting, with sigma = 100.0 s), and (9) Gaussian low-pass temporal filtering (HWHM = 2.8 s). Linear registration of functional to structural scans was carried out using FLIRT (Jenkinson et al., 2002; Jenkinson and Smith, 2001), and nonlinear registration to MNI–152 2 mm isotropic space was conducted with FNIRT (Andersson et al., 2007a,b).

2.3. Seed definitions, nuisance regressor masks, and timeseries extraction

Six striatal spherical seeds (3 mm radii) were created for each hemisphere following the procedures outlined by Di Martino et al. (2008), with centering coordinates adjusted accordingly for MNI–152 2 mm space (see Table 2). The

Table 2
Seed center coordinates in MNI–152 2 mm standard space.

Seed	X	Y	Z
Left dorsal caudate	−12	14	8
Right dorsal caudate	14	14	8
Left dorsal caudal putamen	−28	0	2
Right dorsal caudal putamen	28	0	2
Left dorsal rostral putamen	−24	8	6
Right dorsal rostral putamen	26	8	6
Left ventral rostral putamen	−20	12	−4
Right ventral rostral putamen	20	12	−4
Left ventral caudate	−8	8	−8
Right ventral caudate	10	8	−8
Left nucleus accumbens	−10	14	0
Right nucleus accumbens	10	14	0

seeds included three dorsal seeds within the dorsal caudate, dorsal caudal putamen, and dorsal rostral putamen, and three ventral seeds within the ventral rostral putamen, ventral caudate, and nucleus accumbens (NAcc). Similar to Di Martino et al. (2008), two masks for obtaining nuisance regressor values were created from the Harvard-Oxford Subcortical Structural Atlas. For this study, a ventricular CSF mask was created from atlas voxels with a 75% or greater chance of being classified as belonging to lateral ventricles, and a core WM mask was created from atlas voxels with a 95% or greater chance of being classified as WM. A third nuisance regressor for global signal (Biswal et al., 2010) was calculated as the grand mean of the whole-brain signal. Individual timeseries values were obtained using FSL's *fslmeants*. Global signal timeseries calculations were performed in native space. Timeseries for the six bilateral striatal seeds, CSF mask, and WM mask were created for each subject by FNIRT-based dewarping of the standard-space masks into the native dimensions of the BET-applied fMRI volumes.

2.4. Excess motion correction procedures

Determinations for removal or correction for excess head motion were made following the procedures and recommendations outlined by Power et al. (2012). First, any subject with overall root mean squared (RMS, as output by *3dvolreg*) motion greater than 2 mm was removed from further analyses. Then, three translational and three rotational displacement estimates obtained from *3dvolreg* were combined into Power et al.'s summary framewise displacement (FD) parameter for each volume of each subject's scan. Calculations were performed in R (R Development Core Team, 2012) as an adaptation of the MATLAB code used by Power et al. (2012). Any volume containing or immediately adjacent to a volume with FD > 0.30 was flagged as contaminated by excess motion, and subjects with less than 150 uncontaminated volumes remaining (i.e., subjects with less than 5 aggregate minutes of data) were removed from further analyses. After the RMS- and FD-based corrections, data from 60 subjects were discarded. Compared to the analyzed sample, the dropped participants were younger than the kept participants (dropped M(SD): 18.52(7.19) years, kept: 22.76(6.06) years, $t(164) = 4.05$, $p < 0.0001$). Overall, this study suffered 38.4% data loss (60 of 166 subjects outright, plus a portion of volumes from retained

subjects) from excessive head motion, which is similar to data loss values reported by Power et al. (2012).

2.5. Functional connectivity regressions

FSL's FEAT was used for multiple regression analyses for seeds in each hemisphere, obtaining simultaneous parameter estimates for each hemisphere's striatal seeds while statistically controlling for signal changes within the CSF, WM, and global nuisance masks, as well as for signal changes temporally aligned with the translational and rotational head motion estimates. Additionally, covariates defining the motion-contaminated volumes (as determined by FD calculations) to be "censored" during regression were added on a subject-by-subject basis, with one additional regressor per contaminated volume. Thus, each subject's GLM for each hemisphere had a minimum of 15 parameters (6 seed timeseries, 3 BOLD-based nuisance covariates, and 6 motion-based nuisance covariates), with the potential for additional TR-censoring regressors. At the first level of analysis (iFC estimations for each hemisphere's seeds), correction for time series autocorrelation (pre-whitening) was carried out with FSL's FILM (Woolrich et al., 2001) before all connectivity parameters were estimated.

Because the goal of this study was to examine developmental aspects of dorsal vs. ventral striatal circuits, the six striatal connectivity parameter estimates derived in the first-level multiple regression were combined subsequently in a second-level, within-subject analysis to obtain aggregate fixed-effect estimates for the DS and VS seed regions, as well as DS vs. VS contrasts. This second-level analysis included combinations and contrasts of first-level parameter estimates that assessed mean connectivity effects across the three dorsal seeds (dorsal caudate, dorsal caudal putamen, dorsal rostral putamen); mean connectivity effects across the three ventral seeds (NAcc, ventral caudate, ventral rostral putamen); and difference values for dorsal vs. ventral mean connectivity effects (mean dorsal connectivity greater than mean ventral connectivity, or vice versa). All contrasts combined parameter estimates across hemispheres, given that prior iFC and functional imaging findings indicated similar connectivity patterns for the left and right hemispheres (Di Martino et al., 2008; Postuma and Dagher, 2006).[1] Thus, each subject produced three main statistical maps of interest for entering into the group-level analyses: (1) iFC values for bilateral DS, (2) iFC values for bilateral VS, and (3) iFC difference-values for bilateral DS vs. bilateral VS.

Group-level mixed effects regressions estimating group mean effects for DS iFC, VS iFC, and [DS vs. VS] iFC were carried out with FSL's FLAME and included a dummy-coded scanner variable (representing which scanner was used to collect the data) as a nuisance covariate of no interest. To examine linear and quadratic developmental trends,

---

[1] In separate follow-up analyses (not shown), direct comparisons within this dataset of left and right hemisphere iFC profiles similarly showed that laterality effects were almost exclusively confined to the seeds themselves and immediately adjacent voxels.

additional group mean analyses of the effects of age upon iFC values were carried out with the inclusion of age (linear regression) and age-squared (quadratic regression) covariates. In the linear analysis, the age vector was forced to be orthogonal to the group mean of connectivity. In the nonlinear analysis, the age-squared vector was forced to be orthogonal to both the group mean and to the linear age vector.[2] Correction for multiple comparisons was carried out with cluster-wise thresholding (Worsley, 2001). We used a height threshold of $Z > 2.3$ together with a corrected, whole-brain, clusterwise probability threshold of $p < 0.025$ (i.e., $p < 0.05$, two-tailed). However, for the sake of clarity, we present the findings of the iFC analyses of DS, VS, and [DS vs. VS] effects at a higher threshold (height threshold $Z > 5$; cluster threshold $p < 0.025$) to highlight the strongest regional peaks otherwise hidden among the highly expansive maps of statistically significant iFC values across the whole brain. However, the age-related analyses are presented at the pre-selected threshold of $Z > 2.3$ and $p < 0.025$, as the resultant maps readily cohered into discrete clusters. These analyses provided thresholded Z-score maps of the voxels with significant iFC to the DS and VS seeds, voxels with differential iFC relationships to the DS and VS seeds, and parameter estimates for the effects of age upon striatal iFC profiles.

To further investigate potentially meaningful nonlinear age effects in the regions that were significant in the whole-brain linear age-related analysis, mean iFC values were extracted from anatomically defined regions of interest (ROI) that were represented within the age–iFC voxelwise maps. These extracted iFC values were analyzed using the Statistical Package for the Social Sciences (SPSS), version 22.0. As will be described, four ROIs showed significant age effects in the whole-brain analysis. Each ROI mask (e.g., dorsal anterior cingulate cortex (dACC), left and right anterior insula (laIns; raIns), posterior cingulate cortex (pCC)) was defined by selecting voxels with at least a 50% probability of being classified as the region in question based on FSL atlases. The cingulate mask was further restricted to the dorsal aspect by removing voxels inferior to $Z = 12$, and the insula mask was restricted to the anterior aspect by removing voxels posterior to $Y = 4$. Data extraction was performed via FSL's *featquery*. We then split the sample into three broad age groups to attempt to detect distinct patterns within the age–iFC relationship as a function of age group (Group 1 ($n = 27$): children/adolescents ≤19 y.o., Group 2 ($n = 48$): young adults 19.1–24.9 y.o., and Group 3 ($n = 31$): adults 25.0–44.2 y.o.) (see Table 1 for each age group's demographics). For completeness, we conducted ANCOVAs, controlling for scanner, to assess group differences in iFCs. Furthermore, within each group, we examined the linear vs. quadratic relationships of the significant iFC clusters that were identified in the whole brain analyses of age–iFC correlations. Finally, we conducted exploratory analyses that are reported in

the supplemental material. These exploratory analyses describe mean iFC values across a finer age binning of the sample. Results of these 5-group analyses must be tentatively interpreted because the age distribution across the whole sample is suboptimal for such an approach. But, given our strong hypothesis of unique ontogenic changes in adolescence, we opted for running these additional analyses. Five age groups were thus created: early adolescence (9–13.9 y.o., $n = 8$), mid-adolescence (14–17.9 y.o., $n = 12$), late adolescence (18–24.9 y.o., $n = 55$), early adulthood (25–28.9 y.o., $n = 20$), and early- to mid-adulthood (29–44 y.o., $n = 11$). The supplemental material shows the statistical group comparisons (Supplemental Table S3) and plots of mean iFC for these 5 groups (Supplemental Figure S1), within each significant cluster from the linear age-related whole-brain analyses.

3. Results

We first present DS iFC, VS iFC and [DS vs.VS] iFC across the whole sample, and then the influence of age on DS iFC and VS iFC patterns.

3.1. General patterns of DS iFC (Fig. 2A; Supplementary Table S2)

As expected, positive DS connectivity was observed bilaterally with the prefrontal and frontal motor cortex, anterior cingulate cortex (ACC), as well as the dorsal striatum itself. Positive DS connectivity was also observed within the brainstem and cerebellum. Negative DS connectivity was observed with ventral PFC, NAcc, precuneus, and occipital cortex.

3.2. General patterns of VS iFC (Fig. 2B; Supplementary Table S2)

Positive VS connectivity was observed with ventral PFC, lateral and superior frontal regions, including premotor cortex, ACC, insula, as well as the entire striatum itself. Positive VS iFC also emerged within brainstem and cerebellar regions. Negative VS iFC values were observed with the precuneus, parietal, occipital and temporal regions.

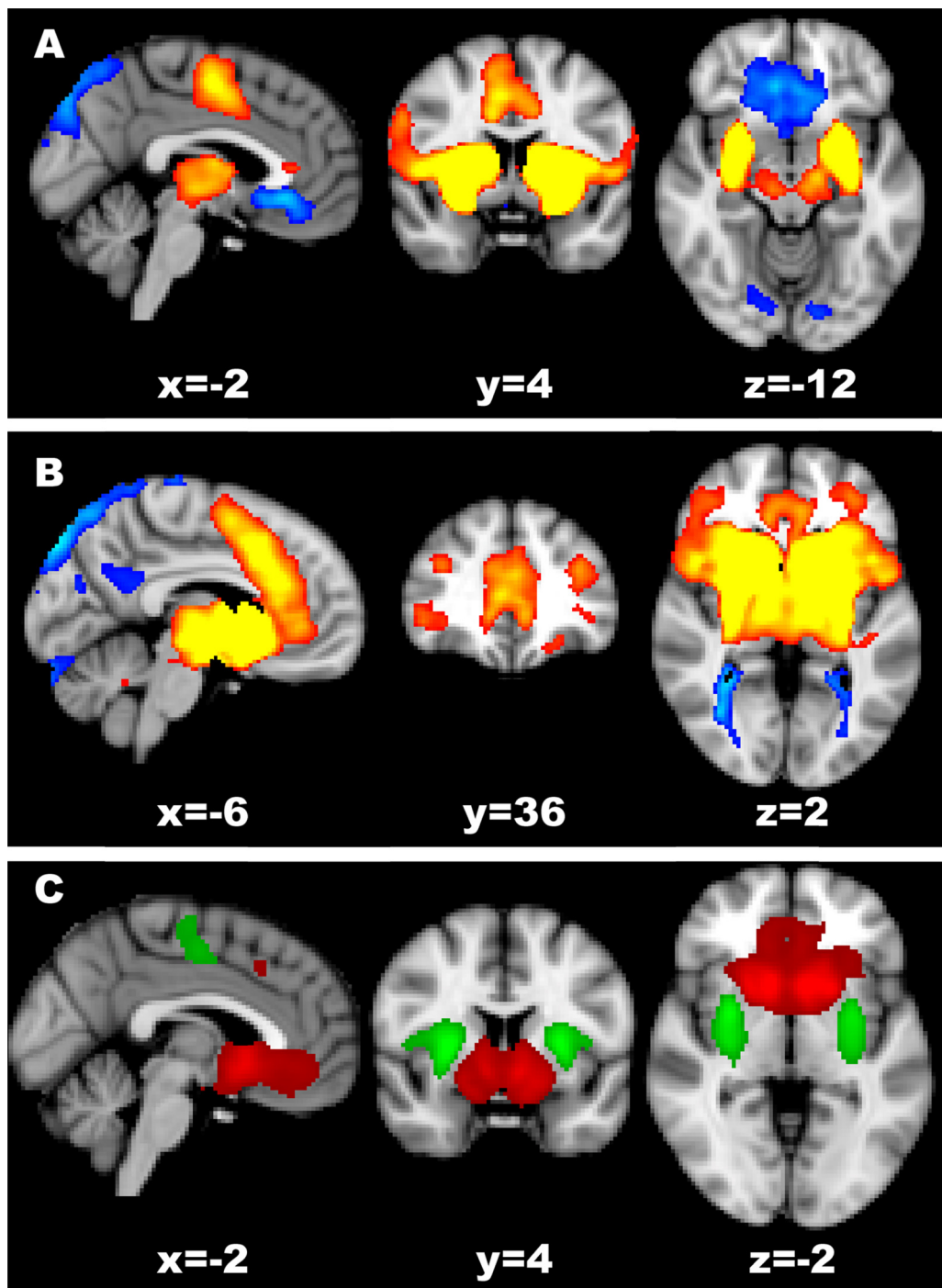### 3.3. Unique patterns of DS iFC vs. VS iFC (Fig. 2C; Table 3)

As expected, medial PFC regions (ventral PFC and ACC) commonly involved in emotion and conflict were connected more strongly with VS than DS, whereas regions implicated in motor and cognitive/attention function (frontal motor strip and parietal cortex) were more strongly connected with DS than VS (Fig. 2C, Table 3). Generally, these differential connectivity patterns for VS and DS cohere with past findings.

3.4. Impact of age on striatal iFC (Fig. 3; Table 4)

3.4.1. Impact of age on DS iFC
The only cluster where age was related to DS iFC was in the posterior cingulate cortex (pCC, peak significance at 6, −20, 44), extending anteriorly into the middle cingulate cortex and posteriorly into the precuneus. Within the

Fig. 2. Striatal iFC patterns. Panel A shows the map for DS iFC (blue = negative iFC; yellow = positive iFC; clusterwise thresholded at $Z > 5$, $p < 0.025$). Panel B shows the map for VS iFC (blue = negative iFC; yellow = positive iFC; clusterwise thresholded at $Z > 5$, $p < 0.025$). Panel C shows the map for the DS vs. VS contrast (red, VS > DS iFC; green, DS > VS iFC; clusterwise thresholded at $Z > 5$, $p < 0.025$). This thresholding across all panels is for visualization only; all analyses were conducted using a clusterwise threshold of $Z > 2.3$ and $p < 0.025$ as described in the text.

whole brain analysis, the correlation with age was positive, indicating greater DS–pCC iFC with increasing age (Fig. 3A). No quadratic trends were observed.

Based on this result, mean regional iFC values within an anatomically defined pCC mask were extracted from

each subject. To better characterize the age–iFC association we compared DS–pCC iFC values across three age groups (Group 1 – children/adolescents ≤19 y.o., Group 2 – young adults between 19.1 and 24.9 y.o., and Group 3 – adults older than 25.0 y.o.) using a univariate ANCOVA,
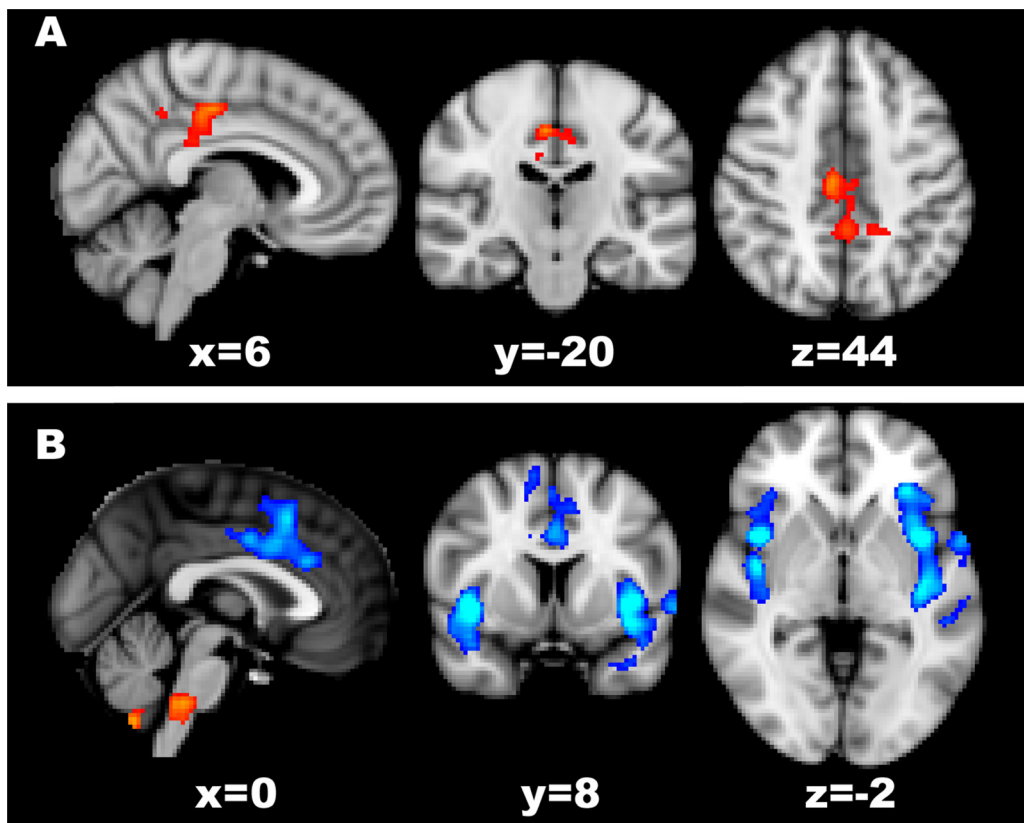
Table 3
Peak values across anatomical areas that are well represented within statistical maps from the contrast of DS iFC vs. VS iFC. Coordinates are in MNI–152 2 mm standard space. Only clusters significant at $Z > 5$, $p < .025$ are presented here despite less stringent thresholding in the analyses. *Abbreviations*: DS, dorsal striatum; VS, ventral striatum; SMA, supplementary motor area; vmPFC, ventral medial prefrontal cortex; iFC, intrinsic functional connectivity.

Cluster	Voxels	Region	X	Y	Z	Peak Z-stat
DS iFC > VS iFC						
		Right putamen	28	0	4	14.26
1	3194	Right caudate	14	14	12	6.99
		Right central operculum	42	−2	12	7.61
		Right parietal operculum	44	−24	16	6.17
2	2592	Left putamen	−30	−2	6	13.51
		Left central operculum	−48	−6	10	7.73
		Left SMA	−2	−10	50	6.65
3	844	Right SMA	6	−10	50	6.61
		Left precentral gyrus	−14	−18	64	5.94
VS iFC > DS iFC						
		Right nucleus accumbens	10	8	−8	19.00
		Left nucleus accumbens	−8	8	−8	17.81
		Right caudate	10	14	0	18.23
		Left caudate	−10	14	0	18.53
1	7516	Right putamen	20	14	−4	15.67
		Left putamen	−18	12	−4	16.63
		Right vmPFC	14	40	−10	8.04
		Left vmPFC	−12	50	−18	5.51
		Right subgenual cingulate	12	32	−6	7.69
		Left subgenual cingulate	−6	32	−6	7.96

controlling for scanner. As expected, age group was a significant predictor of DS–pCC iFC ($F(2,101) = 4.36$, $p = .02$, $\eta_p^2 = .08$). Follow-up contrasts using the LSD method for comparison of means indicated that children/adolescents (≤ 19 y.o.) had significantly lower iFC values than young adults (19.1–24.9 y.o.) ($p = .01$) or adults (>25 y.o.) ($p = .009$). The two latter groups did not differ from one another indicating that DS iFC to the pCC levels off in young adulthood

Fig. 3. Age-related changes in striatal iFC. Panel A shows positive correlations between age and DS iFC in red. Panel B shows positive (red) and negative (blue) age correlations with VS iFC. Both maps clusterwise thresholded at $Z > 2.3$, $p < 0.025$.
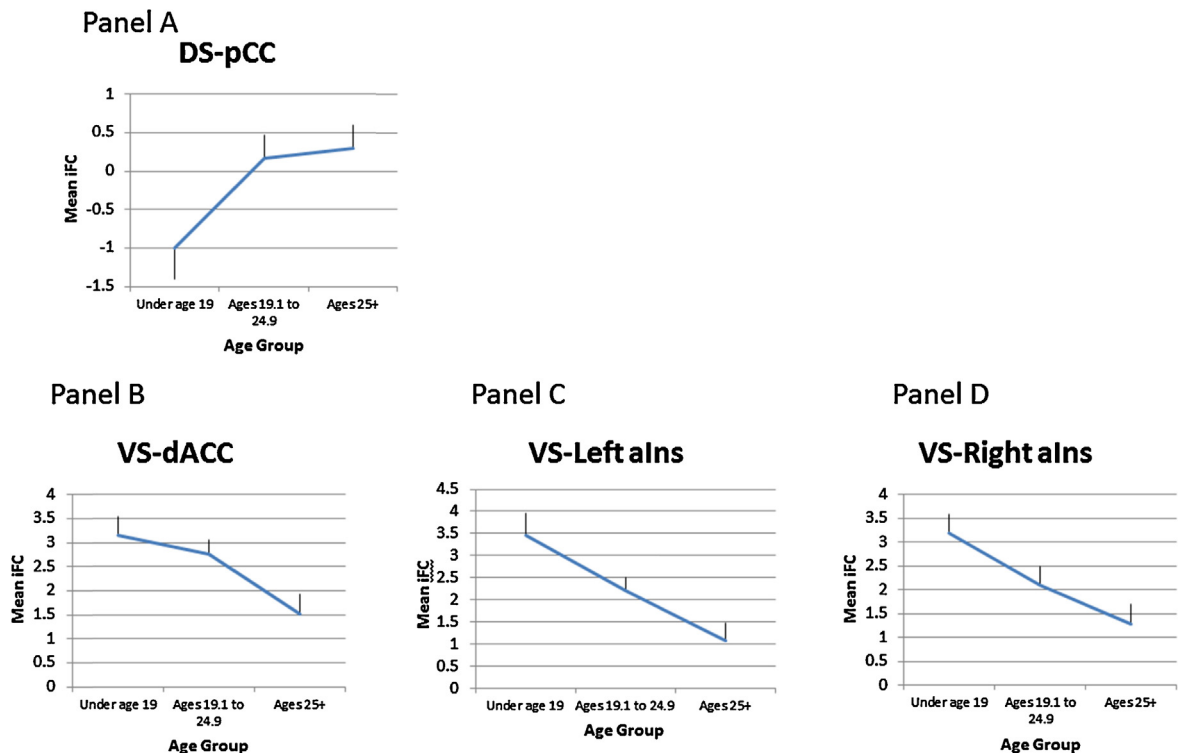
Table 4
Peak values across anatomical regions that are well represented within the statistical maps of age-related changes in striatal iFC. Coordinates are in MNI–152 2 mm standard space. *Abbreviations*: STG, superior temporal gyrus; iFC, intrinsic functional connectivity.

Cluster	Voxels	Region	X	Y	Z	Peak Z-stat
Dorsal striatum						
Age–iFC positive correlations						
		Posterior cingulate cortex	6	−20	44	3.79
1	785	Cingulate gyrus	−8	−14	30	3.37
		Precuneus	−14	−48	50	3.15
Ventral striatum						
Age–iFC negative correlations						
1	1417	Dorsal anterior cingulate	−2	24	26	−3.86
		Paracingulate gyrus	0	16	48	−3.88
		Right insula	42	8	−2	−4.90
		Temporal pole	42	6	−18	−3.45
2	2077	Orbitofrontal cortex	48	22	−12	−3.78
		STG (planum polare)	44	−14	−10	−4.12
		Planum temporale	58	−30	18	−3.57
		Left insula	−40	−4	−8	−4.64
3	3175	Temporal pole	−38	14	−28	−4.31
		Orbitofrontal cortex	−40	22	−12	−4.26
		STG (planum polare)	−46	−16	−8	−4.13
Age–iFC positive correlations						
		Brain stem	−22	−36	−38	3.93
			−6	−40	−42	3.63
1	1460	Cerebellum	10	−50	−44	3.81
			−10	−58	−44	3.46

(19.1–24.9 years) (see Fig. 4A). Second, because each age group is broad, for each age group separately, we conducted linear and quadratic regression analyses on the association of DS–pCC mean iFC values with age. These analyses revealed no significant linear or quadratic associations within each of the three age groups, indicating no evidence of developmental changes in DS–pCC iFC within these more restricted age ranges (Table 5; Fig. 4A).

Fig. 4. Patterns of age and iFC relationships across three age groups (children and adolescents 9–18 y.o., young adults 19–25 y.o., and adults >25 y.o.). Panel A: DS–pCC, Panel B: VS–dACC, Panel C: VS–left aIns, Panel D: VS–right aIns. Values represent mean extracted Z-stat values (±1 standard deviation) from clusters where age exerted a significant influence on iFC. Significant group differences are described in the text. *Abbreviations*: DS = dorsal striatum, VS = ventral striatum, pCC = posterior cingulate cortex, dACC = dorsal anterior cingulate cortex, aIns = anterior insula.

Table 5

Age and iFC partial correlations within each age group. For linear effects, the partial correlations controlled for scanner. For quadratic effects, the partial correlations controlled for scanner and for the linear effect of age. *Abbreviations*: DS, dorsal striatum; VS, ventral striatum; pCC, posterior cingulate cortex; dACC, dorsal anterior cingulate cortex; aIns, anterior insula.

Age group	Age term	DS–pCC	VS–dACC	VS–right aIns	VS–left aIns
Ages 9–19	Linear	.26	.12	.23	−.11
	Quadratic	.12	−.10	−.22	−.11
Ages 19.1–24.9	Linear	.03	.09	.11	.22
	Quadratic	.15	.05	−.06	−.03
Ages 25+	Linear	.05	−.41[*]	−.44[*]	−.54[**]
	Quadratic	.00	−.28	.07	−.30

[*] $p < .05$.
[**] $p < .01$.

3.4.2. Impact of age on VS iFC

In contrast to the single cluster observed for the age effects on DS iFC, three clusters showed significant negative age-related associations with VS iFC: the dorsal anterior cingulate cortex (dACC) extending into paracingulate and supplementary motor area, (peak significance at 0, 16, 48), and the bilateral anterior insula (aIns) (left and right peak significance at −40, −4, −8 and 42, 8, −2) extending anteriorly into the lateral orbital frontal cortex and laterally into superior temporal gyrus as well as into the temporal pole. In addition, VS iFC with brainstem and cerebellar regions increased with age (Fig. 3B; Table 4). No quadratic trends were observed within the whole-brain analysis.

Mean regional VS iFC values within anatomically defined dACC, left aIns, and right aIns masks were extracted from each subject and examined to further characterize the age–VS iFC association. As for the DS iFC analyses, we conducted additional analyses using three age bins. First, as expected ANCOVAs revealed a significant main effect of age group on VS connectivity for each cluster: VS–dACC ($F(2,102) = 5.60$, $p = .005$, $\eta_p^2 = .099$; VS–left aIns $F(2,102) = 9.56$, $p = .000$, $\eta_p^2 = .16$; VS–right aIns $F(2,102) = 8.25$, $p = .000$, $\eta_p^2 = .14$) (Fig. 4B–D). Using the LSD procedure, both the children/adolescents and young adults showed significantly higher VS–dACC iFC than the adult group, and did not differ from each other. This pattern suggests that shifts in VS–dACC iFC take place between early adulthood and middle adulthood after remaining relatively stable through adolescence. Regarding the anterior insula, VS–left aIns iFC differed significantly across all age groups. The children/adolescents showed higher VS–left aIns iFC than the young adults ($p = .023$) or the adults ($p < .001$), and VS–left aIns iFC in the young adults was higher than in the adult group ($p = .011$). A similar pattern was found for the right aIns: children/adolescents showed higher iFC than the young-adult group ($p = .02$) or the adult group ($p = .000$), and the young-adult group showed higher iFC than the adult group ($p = .03$).

We also conducted linear and quadratic regression analyses on the association of VS–dACC, VS–left aIns, and VS–right aIns iFC with age for each age group separately to assess whether quadratic trends might have been obscured in the whole-brain analyses within age ranges of interest. Partial correlations, controlling for scanner, are presented in Table 5; the examination of quadratic effects controlled for the linear effect of age as well as scanner. Within the broad range of adolescence (individuals aged 9–19.0 years)

as well as within young adults (19.1–24.9 y.o.), there were no linear or quadratic effects of age observed for any of the ROIs. However, in adults older than 25 y.o., there were linear declines in VS–dACC iFC as well as linear declines in VS–right aIns iFC.

3.4.3. Exploratory analysis using five age bins (Supplemental Material)

The five age bins covered early adolescence (9–13.9 y.o.), mid-adolescence (14–17.9 y.o.), late adolescence (18–24.9 y.o.), early adulthood (25–28.9 y.o.), and early–mid adulthood (29–44 y.o.). As presented in the supplemental material (Figure S1), visual examination of the 5-age-bin iFC means suggested linear age–iFC relationships for the DS–pCC and the VS–left aIns clusters, but non-linear peaks at mid-adolescence (14–17.9 y.o.) for the VS–right aIns and VS–dACC clusters.

4. Discussion

The goal of this resting state fMRI study was to examine the impact of age on striatal iFC over a period spanning early adolescence into mid-adulthood. Findings are twofold. First, they characterize the iFC of divisions defining aspects of the dorsal–ventral functional dichotomy of the striatum, and second, they reveal differing age–iFC effects within this dichotomy. The age effects provide important novel data informing the dual neural systems model of adolescent motivated behavior.

With respect to the first set of findings, striatal iFC across the whole sample cohered with other reports in adults on iFC patterns for the ventral striatum (VS) and dorsal striatum (DS) (Barnes et al., 2010; Choi et al., 2012; Di Martino et al., 2008). In line with the proposal of a dorsal–ventral striatal functional dichotomy (e.g., Fareri et al., 2008), these resting state studies in adults showed the DS to be more strongly connected with higher cortical association areas in frontal and parietal cortices, and the VS to be more strongly connected with ventral PFC, amygdala, midbrain, and anterior cingulate regions. Here, we showed that the direct comparison of DS iFC with VS iFC confirmed a preferential link of VS to ventral PFC, a region associated with stimulus value coding, emotion processing, and emotion regulation, and of DS to premotor/motor and parietal cortices, regions associated with motor and cognitive processes. This striatal iFC pattern parallels animal and human studies, broadly supporting a role of VS in motivation and emotion, and DS

in motor and cognitive processes (see review, Fareri et al., 2008).

Based on the dual neural systems model of motivated behavior in adolescence, according to which behavioral patterns evolve from two distinct maturational trajectories of motivation and cognitive function (Casey et al., 2008; Luciana et al., 2012; Steinberg, 2010), we predicted that age would differently affect VS iFC and DS iFC, i.e., our second set of findings. In line with predictions, age differentially impacted VS iFC and DS iFC, both qualitatively (location of the target regions), and quantitatively (direction of age effects). Qualitatively, age influenced VS iFC with bilateral anterior insula (extending into orbital frontal cortex) and dACC (extending into supplementary motor area), and DS iFC with pCC (extending into precuneus). Quantitatively, increasing age was associated with decreased VS–aIns and VS–dACC iFC, but with increased DS–pCC iFC.

In addition, exploratory analyses, which are presented in the supplemental material (Figure S1, Table S3), examined extracted regional iFC values according to 5 age groups to tentatively provide a finer representation of age-related changes with age. These exploratory analyses suggested that for VS–right aIns and VS–dACC, there is peak iFC strength (at least nominally; Figure S1) in the 14–17 y.o. group, a finding that could possibly be followed in future work to examine quadratic effects in the adolescent period. However, because these findings are tentative, we will discuss the results according to the whole brain findings of linear associations between age and iFC. Accordingly, the main finding is that VS iFC appears to be high, but DS iFC appears to be low, in adolescents (before age 19 y.o.) compared to adults.

Regarding VS connectivity, the progressively decreasing VS iFC with age in insula and dACC suggests that VS–insula and VS–dACC circuits occupy an important position in the neural (and thus behavioral) repertoire of youths. In other words, based on the putative notion that an iFC network represents the amount of prior use of this network and its readiness to be activated when challenged, and together with previous work (Cho et al., 2013a,b), we reason that communication of VS with insula and dACC serves a unique function in adolescents. Regarding the insula, we recently examined this region in a reward-task-based fMRI study, in which we compared adults with adolescents on a directional connectivity analysis (dynamic causal modeling, DCM) (Cho et al., 2013a,b). The task was the monetary incentive delay task developed by Knutson et al. (2001) to probe striatal function. We modeled a 3-node neural network, encompassing the NAcc of the VS, insula and thalamus. Findings revealed that the insula was significantly involved in the DCM model in response to gains in adolescents, but not in adults, supporting the proposal of a unique role of this region in adolescence. Connections between insula and VS are unidirectional projections from insula into VS. Thus, information processed by the insula, i.e., somatovegetative autonomic signals (Craig, 2009; Paulus and Stein, 2006), is transferred to and used by the VS to code stimulus value and inform actions to be taken. A tighter connection between VS and insula during adolescence might reflect the higher dependence of motivated behavior

on aspects of stimulus salience related to physical arousal. This interpretation is consistent with the description of the more intense emotion and motivational drives experienced by adolescents relative to adults (Cauffman et al., 2010; Crone and Dahl, 2012; Steinberg, 2010; Urosevic et al., 2012).

Similarly, the tighter iFC link between VS and dACC in adolescence suggests that information from VS may shape responsivity of dACC. Information processed by dACC may then loop back to VS and DS (in a spiraling way as described by Haber, 2003), but also be transferred to other regions of cognitive (dorsolateral PFC) and motor control (motor/premotor cortex) (Sallet et al., 2013). Conceivably, this schema might underlie a stronger influence of motivational processes generated at the VS level on executive control and behavioral responses. A similar model has been advanced by Pessoa (2009), who proposed a central role of the anterior cingulate in integrating emotion and motivation signals with executive control processes to generate appropriate behavioral responses. The particularly strong VS–dACC link in adolescence suggests that emotion/motivation, carried by VS, tightly influences dACC activity, which may be implicated in the propensity of adolescent behavior for impulsivity and risk-taking (Steinberg, 2010; Crone and Dahl, 2012). Finally, the reduction in VS iFC strength with age seems to continue beyond the age of 25 years (Fig. 4B), suggesting that motivational networks continue to evolve well into what has generally been construed as young adulthood.

At the same time, increasing age was associated with higher DS iFC with the pCC. The DS–pCC connection in the context of cognitive maturation is highly relevant, and might point to both increased automaticity with age (Packard and Knowlton, 2002), and self-referential cognitive activity (Johnson et al., 2002; Kelley et al., 2002; Vogt et al., 2004). Indeed, adolescents tend to be less prone to stop and reflect when facing emotional situations, and more likely to engage automatically in reactive behavior. In addition, this strengthening of DS–pCC with age seems to taper down after age 19 years suggesting some stabilization of cognitive/motor networks into young adulthood. Collectively, however, this inferential interpretation of the weaker DS–pCC iFC in younger individuals is highly speculative and will need to be supported by behavioral correlates in future work.

Surprisingly, DS–dorsolateral PFC and DS–parietal iFC were not influenced by age in the whole-brain analysis. In fact, findings were still negative (iFC was not modulated by age) when we conducted exploratory ROI-based analyses of the dorsolateral PFC and inferior parietal cortex (data not shown). We would have expected that these networks, thought to support cognitive processes, such as reversal, inhibition, working memory, and attention, would show increased coupling with age, reflecting the age-related improvement in these functions. The present findings suggest that this is not the case. The age-related refinement of these functions might lie in the increased efficiency of local processing (e.g., at the dorsolateral PFC level) rather than improved coupling of the networks, which might be better captured with task-based activation studies. This is an important question both for our understanding of

ontogenic changes, but also of the clinical significance of iFC measures.

Similarly, we were surprised that the amygdala did not emerge in the age-related iFC analyses as a region of interest. VS activity would be modulated by the amygdala, itself under the control of cortical inputs (Ernst and Fudge, 2009). This finding may be particularly important for emotion regulation and impact on behavioral responses during development (Hulvershorn et al., 2014). While the primary VS as well as DS iFC maps do extend into portions of the amygdala, the VS-age clusters that covered the insula did not approach or encompass the amygdala region. Likewise, no age findings were evident in extracted ROI data for the amygdala (post hoc analysis; data not shown).

Collectively, the present findings can also be viewed through the lens of the canonical resting state networks (Damoiseaux et al., 2006; Fox et al., 2005; Laird et al., 2011; Smith et al., 2009), particularly the salience network (Menon and Uddin, 2010) and the default mode network (DMN; Raichle et al., 2001), of which insula and pCC are major hubs, respectively. From this perspective, adolescents are expected to show a stronger VS connection to the salience network, but weaker DS connection to the DMN network. These network dynamics need to be tested more closely using longitudinal designs and corroborated with behavioral measures.

Several limitations of the current study require mention. First, data were obtained from 3 different scanners. However, four factors mitigate this limitation: (1) age was distributed similarly across the 3 scanners; (2) all three scanners were of the same field strength (3T), design model (General Electric Signa), and site of manufacture (Waukesha, WI, USA); (3) the same acquisition sequence was used in all three scanners; and (4) a covariate was used in all group-level GLMs to regress potential systematic signal change related to scanner. A second limitation relates to the 38% of the sample who were removed because of motion artifacts. While these exclusions likely increase the reliability of our findings within this sample, the findings may not fully generalize to individuals with physical or psychological characteristics that impact their abilities to remain still in the scanner. Third, age was not equally distributed across the whole sample, showing fewer subjects at both ends of the 9–44 y.o. age range. This limitation might have prevented us from detecting stronger quadratic relationships between age and striatal iFC. It will be important to replicate the present work in samples that are well populated with younger and older subjects, providing a uniform distribution of age across the sample. Of course, the gold standard would be to conduct a large longitudinal study of healthy subjects. Fourth, study hypotheses were based on models of neural development and striatal function that highlight broad dorsal/ventral distinctions in the striatum. Thus, we did not include more detailed analyses of dorsomedial and dorsolateral striatal circuits involved in habitual vs. goal-directed actions, and which may also exhibit unique age-related changes. This is an area for future investigation. Finally, we lacked behavioral measures to further validate our hypotheses regarding the impact of these intrinsic connectivity patterns on behavioral readiness, particularly with respect to age-related

distinctions in reward processing and executive functioning.

Despite these limitations, our findings do support theoretical views implicating changes in corticostriatal function to explain the behavioral transformations occurring during adolescence. While differences in iFC maps of VS and DS underlie the functional segregation of these two striatal subdivisions, the different effects of age on both regional iFC networks also provides a foundation for understanding behavioral changes with age, in addition to vulnerability to psychopathology. In addition, these findings are based on task-independent activity, which suggests hard-wired endogenous neural interregional dynamics that evolve with age. Taken together, these data provide important insights into the development of intrinsic connectivity patterns and maturation of behaviors subserved by discrete striatal networks.

Conflict of interest statement

The authors declare that they have no competing financial or personal conflicts of interest.

Acknowledgement

Appendix A. Supplementary data

Supplementary data associated with this article can be found, in the online version, at http://dx.doi.org/10.1016/j.dcn.2014.08.011.

References

Alexander, G.E., DeLong, M.R., Strick, P.L., 1986. Parallel organization of functionally segregated circuits linking basal ganglia and cortex. Annu. Rev. Neurosci. 9, 357–381.

Andersson, J.L.R., Jenkinson, M., Smith, S., 2007a. Non-linear Optimisation. FMRIB Centre, Oxford.

Andersson, J.L.R., Jenkinson, M., Smith, S., 2007b. Non-linear Registration Aka Spatial Normalisation. FMRIB Centre, Oxford.

Barnes, K.A., Cohen, A.L., Power, J.D., Nelson, S.M., Dosenbach, Y.B., Miezin, F.M., et al., 2010. Identifying basal ganglia divisions in individuals using resting-state functional connectivity MRI. Front. Syst. Neurosci. 4, 18.

Biswal, B.B., Mennes, M., Zuo, X.N., Gohel, S., Kelly, C., Smith, S.M., et al., 2010. Toward discovery science of human brain function. Proc. Natl. Acad. Sci. U. S. A. 107 (10), 4734–4739.

Bjork, J.M., Knutson, B., Fong, G.W., Caggiano, D.M., Bennett, S.M., Hommer, D.W., 2004. Incentive-elicited brain activation in adolescents: similarities and differences from young adults. J. Neurosci. 24 (8), 1793–1802.

Bjork, J.M., Smith, A.R., Chen, G., Hommer, D.W., 2010. Adolescents, adults and rewards: comparing motivational neurocircuitry recruitment using fMRI. PLoS ONE 5 (7), e11440.

Buckner, R.L., Vincent, J.L., 2007. Unrest at rest: default activity and spontaneous network correlations. Neuroimage 37 (4), 1091–1096, discussion 1097–1099.

Casey, B.J., Jones, R.M., Hare, T.A., 2008. The adolescent brain. Ann. N. Y. Acad. Sci. 1124, 111–126.

Cauffman, E., Shulman, E.P., Steinberg, L., Claus, E., Banich, M.T., Graham, S., et al., 2010. Age differences in affective decision making as indexed by performance on the Iowa Gambling Task. Dev. Psychol. 46 (1), 193–207.

Chein, J., Albert, D., O'Brien, L., Uckert, K., Steinberg, L., 2011. Peers increase adolescent risk taking by enhancing activity in the brain's reward circuitry. Dev. Sci. 14 (2), F1–F10.

Cho, Y.T., Fromm, S., Guyer, A.E., Detloff, A., Pine, D.S., Fudge, J.L., et al., 2013a. Nucleus accumbens, thalamus and insula connectivity during incentive anticipation in typical adults and adolescents. Neuroimage 66, 508–521.

Cho, Y.T., Ernst, M., Fudge, J.L., 2013b. Cortico-amygdala-striatal circuits are organized as hierarchical subsystems through the primate amygdala. J. Neurosci. 33 (35), 14017–14030.

Choi, E.Y., Yeo, B.T., Buckner, R.L., 2012. The organization of the human striatum estimated by intrinsic functional connectivity. J. Neurophysiol. 108 (8), 2242–2263.

Craig, A.D., 2009. Emotional moments across time: a possible neural basis for time perception in the anterior insula. Philos. Trans. R. Soc. Lond. B: Biol. Sci. 364 (1525), 1933–1942.

Crone, E.A., Dahl, R.E., 2012. Understanding adolescence as a period of social-affective engagement and goal flexibility. Nat. Rev. Neurosci. 13 (9), 636–650.

Damoiseaux, J.S., Rombouts, S.A.R.B., Barkhof, F., Scheltens, P., Stam, C.J., Smith, S.M., et al., 2006. Consistent resting-state networks across healthy subjects. Proc. Natl. Acad. Sci. 103 (37), 13848–13853.

Deco, G., Jirsa, V.K., McIntosh, A.R., 2011. Emerging concepts for the dynamical organization of resting-state activity in the brain. Nat. Rev. Neurosci. 12 (1), 43–56.

Di Martino, A., Scheres, A., Margulies, D.S., Kelly, A.M., Uddin, L.Q., Shehzad, Z., et al., 2008. Functional connectivity of human striatum: a resting state FMRI study. Cereb. Cortex 18 (12), 2735–2747.

Ernst, M., Fudge, J.L., 2009. A developmental neurobiological model of motivated behavior: anatomy, connectivity and ontogeny of the triadic nodes. Neurosci. Biobehav. Rev. 33 (3), 367–382.

Ernst, M., Nelson, E.E., Jazbec, S., McClure, E.B., Monk, C.S., Leibenluft, E., et al., 2005. Amygdala and nucleus accumbens in responses to receipt and omission of gains in adults and adolescents. Neuroimage 25 (4), 1279–1291.

Ernst, M., Pine, D.S., Hardin, M., 2006. Triadic model of the neurobiology of motivated behavior in adolescence. Psychol. Med. 36 (3), 299–312.

Eshel, N., Nelson, E.E., Blair, R.J., Pine, D.S., Ernst, M., 2007. Neural substrates of choice selection in adults and adolescents: development of the ventrolateral prefrontal and anterior cingulate cortices. Neuropsychologia 45 (6), 1270–1279.

Fareri, D.S., Martin, L.N., Delgado, M.R., 2008. Reward-related processing in the human brain: developmental considerations. Dev. Psychopathol. 20 (4), 1191–1211.

First, M.B., Spitzer, R.L., Miriam, G., Williams, J.B.W., 2002. Structured Clinical Interview for DSM-IV-TR Axis I Disorders, Research Version, Non-patient Edition. (SCID-I/NP). Biometrics Research, New York State Psychiatric Institute, New York.

Fox, M.D., Snyder, A.Z., Vincent, J.L., Corbetta, M., Van Essen, D.C., Raichle, M.E., 2005. The human brain is intrinsically organized into dynamic, anticorrelated functional networks. Proc. Natl. Acad. Sci. U. S. A. 102 (27), 9673–9678.

Galvan, A., Hare, T.A., Parra, C.E., Penn, J., Voss, H., Glover, G., et al., 2006. Earlier development of the accumbens relative to orbitofrontal cortex might underlie risk-taking behavior in adolescents. J. Neurosci. 26 (25), 6885–6892.

Giedd, J.N., Blumenthal, J., et al., 1999. Brain development during childhood and adolescence: a longitudinal MRI study. Nat. Neurosci. 2 (10), 861–863.

Giorgio, A., Watkins, K.E., Douaud, G., James, A.C., James, S., De Stefano, N., Matthews, P.M., Smith, S.M., Johansen-Berg, H., 2008. Changes in white matter microstructure during adolescence. Neuroimage 39, 52–61.

Haber, S.N., 2003. The primate basal ganglia: parallel and integrative networks. J. Chem. Neuroanat. 26 (4), 317–330.

Harden, K.P., Tucker-Drob, E.M., 2011. Individual differences in the development of sensation seeking and impulsivity during adolescence: further evidence for a dual systems model. Dev. Psychol. 47 (3), 739–746.

Hardin, M.G., Ernst, M., 2009. Functional brain imaging of development-related risk and vulnerability for substance use in adolescents. J. Addict. Med. 3 (2), 47–54.

Hulvershorn, L.A., Mennes, M., Castellanos, F.X., DiMartino, A., Milham, M.P., Hummer, T.A., Roy, A.K., 2014. Abnormal amygdala functional connectivity associated with emotional lability in children with attention-deficit-hyperactivity disorder. J. Am. Acad. Child Adolesc. Psychiatry 53 (3), 351–361.

Jenkinson, M., Bannister, P., Brady, M., Smith, S., 2002. Improved optimization for the robust and accurate linear registration and

motion correction of brain images. Neuroimage 17 (2), 825–841.

Jenkinson, M., Smith, S., 2001. A global optimisation method for robust affine registration of brain images. Med. Image Anal. 5 (2), 143–156.

Johnson, S.C., Baxter, L.C., Wilder, L.S., Pipe, J.G., Heiserman, J.E., Prigatano, G.P., 2002. Neural correlates of self-reflection. Brain 125 (Pt 8), 1808–1814.

Kaufman, J., Birmaher, B., Brent, D., Rao, U., Flynn, C., Moreci, P., et al., 1997. Schedule for affective disorders and schizophrenia for school-age children-present and lifetime version (K-SADS-PL): initial reliability and validity data. J. Am. Acad. Child Adolesc. Psychiatry 36 (7), 980–988.

Kelley, W.M., Macrae, C.N., Wyland, C.L., Caglar, S., Inati, S., Heatherton, T.F., 2002. Finding the self? An event-related fMRI study. J. Cogn. Neurosci. 14 (5), 785–794.

Knutson, B., Adams, C.S., Fong, G.W., Hommer, D., 2001. Anticipation of monetary reward selectively recruits nucleus accumbens. J. Neurosci. 21, RC159.

Laird, A.R., Fox, P.M., Eickhoff, S.B., Turner, J.A., Ray, K.L., McKay, D.R., et al., 2011. Behavioral interpretations of intrinsic connectivity networks. J. Cogn. Neurosci. 23 (12), 4022–4037.

Lebel, C., Beaulieu, C., 2011. Longitudinal development of human brain wiring continues from childhood into adulthood. J. Neurosci. 31 (30), 10937–10947.

Liljeholm, M., O'Doherty, J.P., 2012. Contributions of the striatum to learning, motivation, and performance: an associative account. Trends Cogn. Sci. 16 (9), 467–475.

Luciana, M., Conklin, H., Hooper, C., Yarger, R., 2005. The development of nonverbal working memory processes in adolescents: different maturational trajectories for recall versus executive control. Child Dev. 76 (3), 697–712.

Luciana, M., Collins, P.F., 2012. Incentive motivation, cognitive control, and the adolescent brain: is it time for a paradigm shift? Child Dev. Perspect. 6 (4), 392–399.

Luciana, M., Wahlstrom, D., Porter, J.N., Collins, P.F., 2012. Dopaminergic modulation of incentive motivation in adolescence: age-related changes in signaling, individual differences, and implications for the development of self-regulation. Dev. Psychol. 48 (3), 844–861.

Luna, B., Garver, K.E., Urban, T.A., Lazar, N.A., Sweeney, J.A., 2004. Maturation of cognitive processes from late childhood to adulthood. Child Dev. 75 (5), 1357–1372.

Menon, V., Uddin, L.Q., 2010. Saliency, switching, attention and control: a network model of insula function. Brain Struct. Funct. 214 (5–6), 655–667.

Minino, A., 2010. Mortality among teenagers aged 12–19 years: United States, 1999–2006. NCHS Data Brief 37, 1–8.

O'Doherty, J., Dayan, P., Schultz, J., Deichmann, R., Friston, K., Dolan, R.J., 2004. Dissociable roles of ventral and dorsal striatum in instrumental conditioning. Science 304 (5669), 452–454.

Ordaz, S.J., Foran, W., Velanova, K., Luna, B., 2013. Longitudinal growth curves of brain function underlying inhibitory control through adolescence. J. Neurosci. 33 (46), 18109–18124.

Packard, M.G., Knowlton, B.J., 2002. Learning and memory functions of the basal ganglia. Annu. Rev. Neurosci. 25, 563–593.

Paulus, M.P., Stein, M.B., 2006. An insular view of anxiety. Biol. Psychiatry 60 (4), 383–387.

Pessoa, L., 2009. How do emotion and motivation direct executive control? Trends Cogn. Sci. 13 (4), 160–166.

Postuma, R.B., Dagher, A., 2006. Basal ganglia functional connectivity based on a meta-analysis of 126 positron emission tomography and functional magnetic resonance imaging publications. Cereb. Cortex 16 (10), 1508–1521.

Power, J.D., Barnes, K.A., Snyder, A.Z., Schlaggar, B.L., Petersen, S.E., 2012. Spurious but systematic correlations in functional connectivity MRI networks arise from subject motion. Neuroimage 59 (3), 2142–2154.

R Development Core Team, 2012. R: A Language and Environment for Statistical Computing. R Foundation for Statistical Computing, Vienna, Austria.

Raichle, M.E., MacLeod, A.M., Snyder, A.Z., Powers, W.J., Gusnard, D.A., Shulman, G.L., 2001. A default mode of brain function. Proc. Natl. Acad. Sci. 98 (2), 676–682.

Richards, J.M., Plate, R.C., Ernst, M., 2013. A systematic review of fMRI reward paradigms used in studies of adolescents vs. adults: the impact of task design and implications for understanding neurodevelopment. Neurosci. Biobehav. Rev. 37 (5), 976–991.

Roy, A.K., Shehzad, Z., Margulies, D.S., Kelly, A.M.C., Uddin, L.Q., Gotimer, K., et al., 2009. Functional connectivity of the human amygdala using resting state fMRI. Neuroimage 45 (2), 614–626.

Sallet, J., Mars, R.B., Noonan, M.P., Neubert, F.X., Jbabdi, S., O'Reilly, J.X., et al., 2013. The organization of dorsal frontal cortex in humans and macaques. J. Neurosci. 33 (30), 12255–12274.

Selemon, L.D., Goldman-Rakic, P.S., 1985. Longitudinal topography and interdigitation of corticostriatal projections in the rhesus monkey. J. Neurosci. 5 (3), 776–794.

Smith, S.M., 2002. Fast robust automated brain extraction. Hum. Brain Mapp. 17 (3), 143–155.

Smith, S.M., Fox, P.T., Miller, K.L., Glahn, D.C., Fox, P.M., Mackay, C.E., et al., 2009. Correspondence of the brain's functional architecture during activation and rest. Proc. Natl. Acad. Sci. U. S. A. 106 (31), 13040–13045.

Somerville, L.H., Jones, R.M., Casey, B.J., 2010. A time of change: behavioral and neural correlates of adolescent sensitivity to appetitive and aversive environmental cues. Brain Cogn. 72 (1), 124–133.

Spear, L.P., 2000. The adolescent brain and age-related behavioral manifestations. Neurosci. Biobehav. Rev. 24 (4), 417–463.

Steinberg, L., 2010. A dual systems model of adolescent risk-taking. Dev. Psychobiol. 52 (3), 216–224.

Steinberg, L., Albert, D., Cauffman, E., Banich, M., Graham, S., Woolard, J., 2008. Age differences in sensation seeking and impulsivity as indexed by behavior and self-report: evidence for a dual systems model. Dev. Psychol. 44 (6), 1764–1778.

Urosevic, S., Collins, P., Muetzel, R., Lim, K., Luciana, M., 2012. Longitudinal changes in behavioral approach system sensitivity and brain structures involved in reward processing during adolescence. Dev. Psychol. 48 (5), 1488–1500.

Van Leijenhorst, L., Gunther Moor, B., Op de Macks, Z.A., Rombouts, S.A., Westenberg, P.M., Crone, E.A., 2010. Adolescent risky decision-making: neurocognitive development of reward and control regions. Neuroimage 51 (1), 345–355.

Vogt, B.A., Vogt, L.J., Hof, P.R., 2004. Cingulate gyrus. In: Paxinos, G., Mai, J. (Eds.), The Human Nervous System. Elsevier, San Diego, pp. 915–945.

Voorn, P., Vanderschuren, L.J., Groenewegen, H.J., Robbins, T.W., Pennartz, C.M., 2004. Putting a spin on the dorsal–ventral divide of the striatum. Trends Neurosci. 27 (8), 468–474.

Woolrich, M.W., Ripley, B.D., Brady, M., Smith, S.M., 2001. Temporal autocorrelation in univariate linear modeling of FMRI data. Neuroimage 14 (6), 1370–1386.

Worsley, K.J., 2001. Testing for signals with unknown location and scale in a χ^2 random field, with an application to fMRI. Adv. Appl. Probab. 33, 773–793.